Different responses of the trophic features of particulate organic matter to summer constraints in the Ross Sea

Cristina Misic[1], Anabella Covazzi Harriague[1] , Olga Mangoni [2],

Yuri Cotroneo[3], Giuseppe Aulicino[3], Pasquale Castagno[3]

[1] Dipartimento di Scienze della Terra, dell'Ambiente e della Vita – University of Genova, C.so Europa 26, 16132 Genova, Italy

[2] Dipartimento di Biologia, University of Napoli Federico II, Via Mezzocannone, 8, 80134 Napoli, Italy.

[3] Dipartimento di Scienze e Tecnologie, University of Napoli Parthenope, Centro Direzionale di Napoli IS. C4, 80143 Napoli, Italy

Corresponding author:

Cristina Misic, Dipartimento di Scienze della Terra, dell'Ambiente e della Vita - University of Genova

C.so Europa 26, 16132 Genova, Italy.

Phone: +3901035338224, e-mail: misic@dipteris.unige.it

Abstract

The 0-200 m surface layer of the Ross Sea was studied during summer 2014 to highlight the trophic features of the particulate organic matter (POM) in specific areas. With the aid of satellite information, we selected three zones, characterised by different distances from the coast and different mesoscale hydrodynamic structures: a northern offshore area, crossing the summer-polynya area of the Ross Sea (hereafter called ROME 1), a more coastal area next to the Terra Nova Bay polynya (ROME 2); a southern offshore area, towards the Ross Ice Shelf (ROME 3). Ice-maps showed that the ice retreat had already occurred, leaving general open-water conditions. The statistical analysis of the quantitative features (organic carbon, nitrogen, protein and carbohydrate concentrations) and qualitative trophic characteristics (lability to consumption and caloric value) of the POM pointed to significant differences between the stations, especially in the upper mixed layer (UML). A comparison with other studies previously carried out in the same areas showed that the localised pulses of the POM accumulation in the UML were similar to those recorded at the highly productive marginal ice zones. Therefore, the summer processes could provide significant quantities of materials and energy to the ecosystem, likely also sustaining it in autumn and winter. The UML layer, rather thin and easily subjected to alterations due to global climate change, confirmed its pivotal role in the ecosystem dynamics. A good POM trophic quality was highlighted at several stations in ROME 1 and ROME 3. Reduced trophic support was, instead, found in ROME 2. A proportionally reduced POM consumption in this area, where deep-water formation takes place, would increase the relevance of the POM in the transfer of C to the depths.

Key Words

Antarctica, Ross Sea, physical structure, particulate organic matter, biochemical composition, trophic value

1. Introduction

Particulate organic matter (POM) is composed of a variety of macromolecules and aggregates, whose dimension ranges, arbitrarily, between 0.45-1 µm and 200 µm. POM hosts detrital matter as well as living organisms. Ice-algae, phytoplankton, nano- and microzooplancton, and mesozooplancton-derived particles are included in POM. The presence of phytoplanktonic organisms inside the POM necessitates that its primary ecological role is the foraging of the trophic web in the open sea, where benthic primary production does not occur. On the other hand, the detrital and the heterotrophic microbial components of the POM highlight the fact that this dimensional fraction also has a role in recycling the elements. In addition, POM enters the fluxes of C to the deep waters, taking part to the biological pump that regulates C concentrations in the hydrosphere and atmosphere (Fonda Umani et al., 2002).

In the Antarctic Ocean the quantitative features of the POM have been extensively studied (especially chlorophyll-a, particulate organic carbon - POC - and particulate nitrogen - PN) (Smith et al., 2000; Smith and Asper, 2001), while detailed information on its trophic features is rather scarce. The trophic quality of POM may be studied by means of proxies of its nutritional value. The ratios that are commonly used to infer the trophic value of the POM (for instance the POC/PN ratio and the POC/chlorophyll-a ratio) may be implemented by analyses focusing on its caloric content and on the hydrolysable fractions of the POM (Fabiano et al. 1993; Fabiano and Pusceddu, 1998; Misic and Covazzi Harriague, 2008; Kim et al., 2014). The caloric content expresses the actual value of the POM in energy terms. In this case, different biochemical features generate quantitatively different trophic values for the POM. For the hydrolysable fraction, biomimetic assays have been developed to evaluate the fraction that may be rapidly hydrolysed by the enzymes commonly found in the environment, to calculate the actual fraction of the POM that is bioavailable to consumers. This approach by-passes the uncertainty of bulk-related analyses (such as POC). In fact, the chemical form of the food supply achieves a high relevance for an efficient biological exploitation. The biomimetic assay allows for the possibility that some compounds may be biochemically refractory to consumption, or physically enclosed in low-lability materials that isolate them from consumers.

66 Interannual, seasonal and spatial variability of biological features is typical of the Antarctic Ocean and the
67 Ross Sea (Smith et al., 1996; Arrigo et al., 1998; Dunbar et al., 1998; Gardner et al., 2000; Fragoso and
68 Smith, 2012). However, the mechanisms forcing this spatial heterogeneity are still largely unclear. The
69 presence of ice regulates the onset of primary production, POM accumulation and fluxes in the water
70 column (Garrity et al., 2005). The ice-associated processes physically influence the water column,
71 determining the depth of the upper mixed layer (UML) that is often considered to be a major factor in
72 controlling POM production and distribution (Fragoso and Smith, 2012). Therefore, general trends may be
73 highlighted, based on the degree of maturity of the selected system (Fabiano et al., 2000): closed pack
74 conditions, followed by the Marginal Ice Zone (MIZ) spring conditions, and then by open waters in late
75 spring and summer, generally in the offshore area by late December and in the entire continental shelf
76 region by late January (Comiso et al., 1993, Smith and Asper, 2001). Knowing that ice regulates the
77 biological development and, consequently, the features of the POM, other forces must influence the
78 planktonic patterns when ice is lacking, during summer for instance. Although ice may last longer at some
79 sites in the Ross Sea, depending on global climate anomalies as well as local events (Arrigo and van Djiken,
80 2004), the summer features of the Ross Sea should show less variability than the spring ones. The
81 stratification generated by ice melting should be relaxed due to wind and waves on the open waters, a
82 feature that would allow increased vertical fluxes and a more homogeneous vertical distribution of the
83 POM (Gardner et al., 2000).
84 This study is based on the results of the ROME (Ross Sea Mesoscale Experiment) cruise, carried out during
85 the Antarctic summer of 2014. Sampling was performed focusing on the 0-200 m surface layer of three
86 areas of the Ross Sea, characterised by different distances from the coast and different mesoscale
87 hydrodynamic structures.
88 We aimed to: i) highlight whether the quantitative and qualitative features of the POM were homogeneous
89 in the sampled areas, ii) test whether our summer POM features resembled those of previous research
90 performed in the Ross Sea, iii) underline the potential role of the POM in the trophic exchanges and in the
91 global carbon trends of the area.

2. Material and methods

2.1 Station sites and sampling

The in situ ROME data were collected by the R/V Italica in the framework of the Italian National Program for Antarctic Research (PNRA). Sampling was performed in three different areas of the Ross Sea: ROME 1 was sited at approximately 170°E and 75°S; ROME 2 occupied a more coastward area, next to the Terra Nova Bay (TNB) polynya; ROME 3 was sited in the southern Ross Sea, towards the Ross Ice Shelf, at 168°E (Fig. 1A).

The sampling strategy was defined on the basis of the MODIS (Moderate Resolution Imaging Spectroradiometer) Aqua and Terra satellite level-2 products for the previous 12/24 hours. In particular, the sea surface temperature and surface chlorophyll-a concentration maps at 1 km resolution were analyzed in order to plan and to carry out the casts in correspondence with both high and low chlorophyll signals. Additionally, satellite AMSR2 sea ice concentration maps, provided by the University of Bremen, using the ASI sea ice concentration algorithm (Spreen et al., 2008), were considered. In fact, daily maps of the Ross Sea region from early December 2013 to late February 2014 (available at http://www.iup.uni-bremen.de:8084/amsr2) were analyzed to monitor the evolution of the sea ice cover before and during the experiment, in order to study its effects on the physical and biochemical systems.

A total of 46 casts were obtained. Hydrological profiles were acquired by means of a SBE 9/11 Plus CTD, with double temperature and conductivity sensors. For each station the upper mixed layer (UML) depth was determined as the depth at which *in situ* density (σ_t) changed by 0.05 kg/m^3 over a 5 m depth interval. Current speed and direction were recorded using a Lowered Acoustic Doppler Current Profiler (LADCP) system. Two LADCP were deployed with a CTD, to obtain a unique current measurement every 10 m from the surface to the maximum depth reached. The effect of tides on this current dataset was removed following the procedure proposed by Erofeeva et al. (2005).

The POM sampling was performed at 21 stations (Table 1, black circled stations in Fig. 1A) using 12-L Niskin bottles. Samples were collected at 4 fixed depths (surface, 50, 100 and 200 m) and 1 variable depth

118 depending on the maximum of the signal for fluorescence. From 0.5 to 1 L of sampled seawater was filtered
119 through Whatman GF/F filters (nominal pore diameter 0.7 μm), and immediately frozen until analysis in the
120 laboratory.
121
122 *2.2 Analytical procedures*
123 The filters for the spectrofluorometric analyses of the chlorophyll-a and phaeopigments were stored at –
124 80°C and analyzed with a Varian Eclipse spectrofluorometer, following Holm Hansen et al. (1965). The
125 instrument was checked daily with a chlorophyll-a standard solution (from *Anacystis nidulans* by Sigma).
126 The specific standard deviation of the replicates was on average 4%.
127 Particulate organic carbon (POC) and particulate nitrogen (PN) were analyzed following Hedges and Stern
128 (1984), after acidification with HCl fumes in order to remove inorganic carbon. Cyclohexanone 2-4-
129 dinitrophenyl hydrazone was used to calibrate a Carlo Erba Mod. 1110 CHN Elemental Analyser. The
130 specific standard deviations due to the analytical procedures and sample handling were 7.4% and 7.8% for
131 POC and PN, respectively.
132 Particulate proteins, particulate carbohydrates and particulate lipids were analyzed following Hartree
133 (1972), Dubois et al. (1956), Bligh and Dyer (1959) and Marsh and Weinstein (1966). Albumin, glucose and
134 tripalmitine solutions were used to calibrate a Jasco V530 spectrophotometer. The specific standard
135 deviations were 8.3%, 15.5% and 21.6% for the proteins, carbohydrates and lipids, respectively.
136 Besides the quantitative information given by the single concentration of the different elements and
137 biochemical types, the POC/PN ratio (Huston and Deming, 2002) and the particulate protein/carbohydrate
138 ratio (Misic and Fabiano, 1996) gave clues to the qualitative value of the POM for the consumer. The lower
139 the POC/PN and the higher the protein/carbohydrate ratio, the higher the trophic value of the POM.
140 The concentrations of proteins, carbohydrates and lipids were used to calculate the caloric value of the
141 POM (Kcal g POM^{-1}) following the Winberg (1971) equation (Kcal g POM^{-1} = 0.055 protein% +0.041
142 carbohydrate% + 0.095 lipid%).

143 The hydrolysable particulate proteins and carbohydrates were determined following the protocols of
144 Gordon (1970), Mayer et al. (1995) and Dell'Anno et al. (2000). The sample filters and filter blanks
145 (Whatman GF/F filters not used for filtration) were placed in plastic containers with solutions (100 mg l^{-1} in
146 0.1 M Na-phosphate buffer) of two selected enzymes purchased from Sigma–Aldrich. Proteinase K was
147 chosen for the hydrolysis of the proteins, β-glucosidase for that of the carbohydrates. These enzymes are
148 extracted from plants and fungi, but have hydrolytic activities quite similar to natural marine organisms and
149 are widespread among autotrophs and heterotrophs (Dall and Moriarty, 1983). The filters were left in the
150 enzyme solutions for 2 hours, at the optimal temperatures and pH for each enzyme in order to enhance the
151 digestion. After hydrolysis, each filter was carefully removed from its container, placed in a filter-holder and
152 rinsed with the solution remaining in the dish and 5ml of deionised water to return any particles that may
153 have floated off the filter. Then the filters were processed for the determinations of proteins and
154 carbohydrates following the same protocols as above. The possibility that the flushing of the buffer could
155 have mechanically removed part of the particulate fraction was avoided by incubating and processing
156 replicates of the samples with only the buffer solution. The concentrations detected after hydrolysis,
157 corrected for the eventual error just mentioned (never higher than 20% of the total protein and
158 carbohydrate concentrations), were subtracted from the total concentrations in order to obtain the
159 hydrolysable, or labile, POM. The specific standard deviations were 11.2% and 21.5% for hydrolysable
160 particulate proteins and carbohydrates, respectively.
161
162 *2.3 Data treatment and statistical analysis*
163 The data were divided into a surface layer and a deeper layer, the former defined by the UML depth (Table
164 1) and the latter ranging from the UML depth down to 200 m.
165 The literature data related to previous research carried out in the Ross Sea and TNB were utilised as a
166 comparison. For the Ross Sea Fabiano et al. (2000) provided spring data and Fabiano et al. (1993) and
167 Catalano et al. (1997) early summer data. Fabiano et al. (1995 and 1997) and Povero et al. (2001) provided
168 summer data for the TNB area (Table 2).

We tested the differences of the same variable between different samplings with the one-way ANOVA test followed by the Newman-Kneuls *post-hoc* test (ANOVA-NK test) (Statistica software). To test the relationships between the various parameters, a Spearman-rank correlation analysis was performed.

The Principal Component Analysis (PCA) was applied to the normalised data of the POC, protein and carbohydrate concentrations and the protein/carbohydrate ratio (PRIMER software). The data were divided into the UML and the deeper layer, as previously described. The ROME data were treated together with the other literature data previously cited (Table 2) to highlight similarities between them. The analysis of similarities (ANOSIM) was applied to highlight significant differences between the groups identified by the cluster analysis performed on the normalised data (resemblance measure: Euclidean distances, cluster mode: group average), while the similarity percentage analysis (SIMPER) was utilised to highlight the parameters responsible for such differences.

3. Results

3.1 Physical properties and sea-ice conditions

The Θ/S diagram obtained from all the sampled stations (Fig. 1B) indicated the presence of several typical Ross Sea shelf water masses. In all the areas studied the surface layer was occupied by the Antarctic Surface Water (AASW), a relatively light surface water characterized by potential temperatures ranging between -1.8°C and +1°C and by salinity values lower than 34.50 (Orsi and Wiederwohl, 2009). According to previous studies (Orsi et al., 2009), a westward increase in salinity was evident in this layer. In ROME 2 (blue circles in Fig. 1B), the AASW core was slightly saltier, colder and denser than expected, with salinity close to 34.60 and potential density lower than 27.9 kg/m^3. These values were similar to the Modified Circumpolar Deep Water (MCDW) features, but the high oxygen concentration values (Rivaro et al., this issue) confirmed that we were in the presence of a local AASW. Moreover, both in ROME 1 and ROME 2, isolated high temperature values (> 1°C) were episodically observed in the first 35 m depth, probably due to summer insulation.

194 The intermediate and deep layers (from 150 to 1000 m) were occupied by High Salinity Shelf Water (HSSW),
195 and by Terra Nova Bay Ice Shelf Water (TISW), the latter identified only in ROME 2 (Fig. 1B). HSSW is
196 characterized by salinity greater than 34.70, potential temperature near freezing point and potential
197 density greater than 27.9 kg/m^3 (Budillon et al., 2003; Rivaro et al., 2014). TISW is a local expression of the
198 typical ISW, characterized by potential temperatures below freezing point and salinity values of about
199 34.70 (Budillon and Spezie, 2000). It was located in the 150-350 m layer and was the coldest water mass
200 identified during the experiment.
201 The physical properties of the upper layer may also be linked to sea ice evolution in the study area. The ice
202 melting in the Ross Sea gradually generates large ice-free areas during summer. Some ROME 1 and ROME 3
203 stations and all the ROME 2 stations experienced ice-free conditions starting from early December (Figs. 2A
204 and 2B). On the other hand, some stations experienced the presence of ice longer (Figs. 2C and 2D). Even in
205 the same sampling area, differences in ice cover can be significant and have an impact on the observed
206 temperature and salinity values. For instance, the northernmost station of ROME 1 (station 20) was
207 covered by ice until 14 January, just 3 days before the sampling. Stations 16 and 18 began to become ice-
208 free from the beginning of January (Fig. 2C). The ROME 3 stations were partially covered by ice until the
209 end of December, namely by the ice barrier lying between the Ross Sea summer polynya and the Ross
210 Island coastal opening (Fig. 2B).
211 The vertical structure of the water column of ROME 1 showed deeper UMLs for the stations that
212 experienced longer ice-free conditions (9, 11 and 13, Table 1). In the western stations of ROME 1 the lower
213 depth of the mixed layer depended on the presence of low-salinity surface water, related to the influence
214 of the ice (Fig. 3B). Intensity and direction of the currents in the UML (Fig. 3D) showed the presence of a
215 northward current along the eastern and western boundary of the leg, while more intense southward
216 velocities were registered in the central part of the leg (stations 13 and 14). This pattern was confirmed for
217 the entire water column (not shown).
218 The ROME 2 water column presented some peculiar features. The surface layer was characterized by a
219 temperature and salinity gradient between the fresher and colder coastal stations and the easternmost,

220 saltier and warmer stations (Figs. 4B and 4C). These hydrographical conditions limited the UML depth to
221 the first 10-15 m for all the sampled sites except stations 33 and 39, which had a slightly deeper UML (Table
222 1). A frontal structure was visible in the area between stations 45 and 34, where the convergence of the
223 two water masses led to a deepening of the thermocline down to 100 m (Rivaro et al., this issue). Stations
224 33 and 39 were separated from the coast by the front and showed features more similar to the offshore
225 stations. The differences between the coastal and offshore waters were also evident in the current pattern,
226 which made an abrupt change in direction along the frontal area, where intense southward velocities were
227 registered (Fig. 4D).
228 The strongest current intensities ($p<0.05$) were observed in ROME 3, with values up to 24 cm sec^{-1} for the
229 zonal (u) and meridional (v) components. The current pattern at all depths showed the presence of a
230 cyclonic circulation centred at about 168.5°E 76.45°S (Fig. 5D). This circulation could have increased the
231 UML water mixing, leading to salinity values of 34.23-34.43 and mean temperature values lower than 0.5°C
232 (Figs. 5B and 5C). In fact, the western and central stations (48, 50, 55, 67 and 75) had a more homogeneous
233 water structure for the upper 30-50 m, while stations 52 and 65, placed outside the eddy at the eastern
234 side of the sampling area, showed higher surface salinity values and the deepest UML (more than 70 m).
235
236 *3.2 Particulate organic matter*
237 The concentration and distribution of chlorophyll-a in the three areas (Table 3) varied, depending on the
238 physical constraints. In ROME 1 the stations characterised by early ice melting showed deeper mixed layers
239 and rather homogeneous chlorophyll-a concentrations in the UML, ranging from 1 to 2 µg l^{-1}. On the other
240 hand, where the alocline was shallower and the stratification stronger (i.e. station 16), a subsurface
241 increase in concentration up to 3 µg $l^{-1}$was observed, leading to higher average values (Table 3).
242 The chlorophyll-a distribution in ROME 2 was influenced by the previously described hydrological front,
243 associated with the deepening of the thermocline at stations 34 and 45. The frontal structure and the
244 current convergence allowed high chlorophyll-a concentrations at higher depths (values up to 3 µg l^{-1} at
245 100 m, data not shown).

246 The UML at stations 55, 67 and 75, in ROME 3, directly influenced by the cyclonic eddy, showed the highest
247 mean chlorophyll-a concentrations (Table 3), with maximum values higher than 4 μg l^{-1}.
248 The POC values correlated significantly with the chlorophyll-a ones in ROME 1 and ROME 3 (Table 4). ROME
249 2, instead, showed no significant correlation. ROME 2 was, however, significantly richer ($p<0.05$) than the
250 other two at 50 and 100 m depths (Fig 6A).
251 The POC/chlorophyll-a ratio indicates the primary biomass contribution to the total POM, the lower the
252 value the higher the phytoplanktonic contribution (Fonda Umani et al., 2002). The ratio values (Table 3)
253 highlighted a generally lower contribution of the photoautotrophic component at the UMLs of ROME 1 and
254 2, with ratio values higher than 150. In ROME 1 the stations experiencing longer ice-free conditions
255 (stations 9 and 11, for instance) showed the highest ratio values in the entire mixed layer, and station 52 in
256 ROME 3 also showed the same features. At the other stations in ROME 1 and 2 the ratio decreased with
257 depth, reaching its lowest values (ratio near 50) at station 34. In ROME 3 the lowest ratio values were,
258 instead, found in both the surface and subsurface layers, especially for the stations lying to the west of the
259 frontal zone.
260 Although the PN and POC concentrations were strongly correlated (Table 4), indicating similar distributions
261 (Figs. 6A and 6B) and, possibly, origin, the POC/PN ratio values showed variations with depth (Fig 6C). The
262 POC/PN ratio gives an estimate of the N contribution to the bulk POM, keeping in mind that N-containing
263 molecules are considered attractive to consumers (Huston and Deming, 2002). The highest POC/PN ratio
264 values (above 8) were found in the deeper water layers, especially at stations 9 and 11 in ROME 1 and 50,
265 52, 56, 69 and 75 in ROME 3. The lowest values, below 6, were, instead, found in the UML, especially in
266 ROME 3, where the highest chlorophyll-a values were found. However, significant chlorophyll-a and
267 POC/PN ratio correlations were only found in ROME 2, although this relationship ($r= 0.48$, $n=19$, $p<0.05$)
268 highlighted that an increase of autotrophic biomass led to a lowering of the trophic value of the POM.
269 On average, the protein and carbohydrate concentrations showed vertical trends very similar to the POC
270 ones (Figs. 6D and 6G). This was also confirmed by the significant correlations found between these
271 variables for the three areas (Table 3). Proteins and carbohydrates correlated also with chlorophyll-a in

ROME 1 and 3, while no significant correlation was found in ROME 2. Furthermore, the hydrolysable fraction of the carbohydrates and lipids was not coupled with the other variables in ROME 2 and a reduction of the hydrolysable carbohydrates was, in fact, observed starting from 100 m (Fig. 6H). In this area the lipid concentrations (Fig. 6I) did not show significant decreases with depth (UML vs. deeper layer, $p>0.05$) but rather similar values, significantly lower than in the other areas ($p<0.001$).

On average, the hydrolysable proteins were 35.4±11.7% of the total proteins (ranging from 6.8 to 75.6%), the hydrolysable carbohydrates 13.1±10.8% of the total carbohydrates (ranging from 0.1 to 44.9%). Generally the deeper layer percentages were higher than the UML ones, except for the front-related stations in ROME 2 and station 20 in ROME 1. This was also true considering the sum of the contribution of hydrolysable proteins and carbohydrates to the POC (Fig 7).

3.3 Multivariate statistical analysis

Fig. 8 reports the PCA plot, where the cluster analysis results are shown as ellipses defined by Euclidean distances. The PC1 axis explained 71% of the variation, while the PC2 explained a further 24% of the variation. Two significantly different main groups (ANOSIM analysis, Table 5) were observed: the UML observations belonged to the richer group A, with the exception of the closed-pack, the early summer polynya observations, station 20 of ROME 1 and station 34 of ROME 2. Those observations were grouped together with all the deeper-layer observations in group B. Proteins and carbohydrates explained the major part of this difference (SIMPER analysis, Table 5). The group B stations showed POC concentrations 3.4-fold lower than the observations of group A, 4.8 for proteins and 2.8 for carbohydrates.

In group A the samples were organised into two main sub-groups: a1 and a2. The multivariate analyses highlighted significant differences between these sub-groups (ANOSIM analysis, Table 5), mainly due to the different ratios between proteins and carbohydrates (explaining 41% of the difference, SIMPER analysis, Table 5). In group B two more sub-groups were recorded, differing significantly (ANOSIM analysis, Table 5) due to the carbohydrate concentrations (explaining 47% of the difference, SIMPER analysis, Table 5).

297 Each sub-group had a particular signature, defined by the previous studies carried out in the area (Table 2):
298 sub-group a1 clustered the MIZ stations (8, 10, 28, 30) and the spring polynya station MP, sub-group a2 the
299 coastal TNB stations. The surface observations characterised by a closed-pack coverage (27 and 29)
300 belonged to sub-group b1, together with the main part of the deeper layer observations; sub-group b2
301 collected those of the early summer polynya stations (15, 17, 19, 21) and the deeper coastal layer
302 observations (TNB).
303
304 *3.4 Caloric value analysis*
305 The caloric value of the POM in the two water layers was only calculated for those stations where the lipid
306 analysis was carried out, namely 9, 13, 16 and 20 of ROME 1, 34, 39 and 45 of ROME 2 and 50, 55 and 67 of
307 ROME 3. The plot of these results, with the previous research carried out in the Ross Sea and at the coastal
308 TNB (Table 2) is presented in Fig. 9. In this figure we have merged the bulk quantitative (POC) and
309 qualitative (caloric value) information on the POM.
310 Previous research highlighted a rising trend of the quantitative features in the UML, from the poorer pack-
311 ice zones to the polynya and then to the MIZ, ending with the richer coastal sites, although the MIZ could
312 also show high concentrations of POM of moderate caloric values. The previous pack-ice observations
313 showed that low concentrations were associated with an average caloric value, especially at the northern
314 station 27, while the qualitative value of the other stations was higher (MIZ and coastal) or lower (polynya).
315 The observations of the deeper layer of the MIZ and of the spring-early summer polynya showed similar
316 features to areas influenced by pack-ice, while the coastal observations had higher quantitative and
317 qualitative characteristics.
318 The stations in ROME 2 matched the quantitative and qualitative features of the polynya in the entire water
319 column. The surface observations of the other areas were grouped with the MIZ and previous coastal
320 observations for the UML. The deeper layer observations in the ROME 1 and ROME 3 areas resembled
321 those of the MIZ, spring polynya and deeper pack-layer, although their caloric value was higher.
322

4. Discussion

4.1 Quantitative and qualitative trophic features of the summer POM: a comparison with previous studies in the Ross Sea

The study of the features and role of the POM in the ecosystem may be approached at different levels. The first level we tested was focused on the quantitative characteristics of the stations (PCA multivariate analysis, Fig. 8). Although the UML was rather thin at several stations, significant quantitative differences were observed between the two water layers (Table 5), with a sharp reduction in POM in the deeper layer, already established by the observations by Nelson (1996), Fabiano et al. (2000) and Gardner et al. (2000) for the Ross Sea. They stated that the primary production is recycled in the photic layer and only a small part (less than 20%) will sink to the bottom, following the concept of a "retentive system". The grouping of the observations of the two layers, as revealed by the multivariate analysis, indicated a stronger and significant variability in the UML, while the deeper layer was rather homogeneous, also when compared to observations from other years and seasons.

Except for the northern stations of ROME 1 (18 and 20), ice-free water conditions were established in the whole ROME sampling area starting from the beginning of January, at least two weeks before the sampling. Open water conditions, resembling those of the previous spring-summer polynya/open water observations used as a comparison (Table 2), should then be common. The multivariate analysis indicated polynya/open-water features for the UML, but many were also similar to the previous MIZ observations.

The sub-group a1 linked some stations of the ROME cruise and the previously studied spring polynya station MP. Nevertheless, Fabiano et al. (2000) observed that this station was part of a more complex period of melting-ice. This may explain why this station was also grouped with the spring MIZ ones in the PCA plot. The MIZ stations were generally characterised by high POM productivity (Saggiomo et al., 1998; Fitch and Moore, 2007), being the priming for further planktonic development. The multivariate statistical analysis indicated that these stations showed rather high POM concentrations and, in particular, the highest prevalence of proteins over carbohydrates. It is well known that N-rich proteins cover multiple roles (energy, functional, plastic) and thus they are proxies of good trophic value POM (Etcheber et al., 1999).

Particulate carbohydrates, instead, generally have a lower trophic quality, because they are composed by complex structural polysaccharides whose digestion is highly energy-consuming. One of the main processes that enrich the POM of proteins is microbial activity. Microbial heterotrophic reworking of autotrophic and detrital POM, generally performed by bacteria, increases the N content of the detritus (Povero et al., 2003) and of the autotrophic colonies (Carlson et al., 1998) especially during summer. A general and marked dominance of proteolysis over other classes of hydrolytic enzymes has been previously reported (Misic et al., 2002; Celussi et al., 2009), indicating an efficient N-recycling by unicellular heterotrophs. The conversion of detrital-N into high trophic value biomass is completed by an efficient microbial-loop, recovering a large part of the DOM released during phytoplanktonic blooming (Kirchman et al., 2001). In addition, Sala et al. (2005) found that bacteria might utilise other DOM sources (in particular dissolved carbohydrates), thus increasing their efficiency in biomass accumulation.

Another process that may increase the protein concentration is the blooming of phytoplankton with a high constitutive protein content. For instance, in cold waters the diatom protein content is approximately double that of temperate waters, which results in a low POC/PN of approximately 5 (Young et al., 2015). The very high chlorophyll-a concentrations of some of these stations (48, 56 and 75 for instance) agree with this second hypothesis and bring these stations closer to the highly productive spring season.

The other UML observations of the ROME cruise (sub-group a2) resembled the coastal features of TNB during summer, showing the highest concentrations of POM, although their trophic quality was lower than that of sub-group a1.

These concentrations may depend on heterotrophic as well autotrophic activity. For instance, the long-term ice-free stations of ROME 1 (9 and 11) showed a heterotrophic signature (high POC/chlorophyll-a ratio values), indicating the relaxing of the primary production or an overwhelming activity of metazoans that prevented the accumulation of the autotrophic biomass. Grazers and predators would take up the POM resources and release trophically-depleted residuals, as indicated by the POC/PN ratio values of approximately 8 in the deeper layer of these stations, and as observed by Huston and Deming in the Arctic (2002).

In the Ross Sea the autotrophic processes occurring during summer could provide a large accumulation of biomass, strongly sustaining the ecosystem. This feature was not clear in the multi-year comparison by Arrigo and van Djiken (2004) and in the studies by Smith and Asper (2001) and Rigual-Hernandez et al. (2015), who observed a general decrease of chlorophyll-a concentrations from spring to summer in normal years.

The study of the ROME 3 results may help to explain the reasons for these highly productive features. The results obtained during this cruise provided a good example of the relationships between physical forcing, phytoplanktonic biomass and POM accumulation. In this case the UML depth (generally deeper than 30 m) exerted a lower influence on the POM production and accumulation than that observed by Fragoso and Smith (2012), who noted that the shallower mixed layer depths (<20 m) in late spring and early summer appeared to promote diatom growth. The phytoplanktonic biomass was absolutely pivotal for the POM composition. In fact, it regulated the POM quantitative features, as revealed by the highly significant correlations between the chlorophyll-a and the quantitative variables of the POM (Table 4) (Davis and Benner, 2005) and by the POC/chlorophyll-a ratio values for the stations on the western side of the area (eddy-influenced zone), that were significantly lower ($p<0.05$) than the other ROME areas. Young et al. (2015) found that Antarctic diatoms should devote up to 50% of biomass to protein, explaining the very high significance of the correlation. Arrigo and van Djiken (2004) described the area of ROME 3 as a boundary between spring blooms and summer blooms. A sort of frontal area, that may show an unusually high chlorophyll-a accumulation at the surface, depending on general atmospheric conditions over the entire Ross Sea. The blooming we observed was influenced by the peculiar physical constraints of this area, such as the presence of a frontal area and a cyclonic eddy that divided some of the richer north-western stations from the others. The water mixing of the UML, due to the more intense hydrodynamic forcing, fertilised the surface layer, probably stripped of nutrients by earlier spring blooms. On the other hand, a higher instability in the water column, that is known to influence phytoplanktonic development, could have favoured some species that, before, were limited by competition (Fonda Umani et al., 2002).

400 The last sub-group showing polynya features is the b2 of the PCA. In this group station 20 of ROME 1
401 matched the features of the early summer polynya stations, despite the fact that it was ice-free for a
402 shorter time than the others. Horizontal advection of POM from the adjacent areas could have provided
403 the concentrations we found (Rigual-Hernández et al., 2015). The heavier ice-influence could have favoured
404 the accumulation and persistence of sympagic-derived materials, as indicated by the rather high surface
405 chlorophyll-a concentrations.
406
407 *4.2 Caloric value of summer POM*
408 The plotting of the POC with the POM caloric value (Fig. 9) provides information on the energy potentially
409 provided to heterotrophic consumers by the POM.
410 The ROME stations that qualitatively resemble the spring and early-summer features of the polynya were
411 those of ROME 2. Actually, these stations experienced real polynya environmental conditions, being next to
412 the TNB polynya. The ROME 2 stations, in fact, had low caloric values in the entire water column, although,
413 from a quantitative point of view, some of them in the UML had similar features to the richer coastal areas
414 (sub-group a2 of Fig 8). Low current velocities and a peculiar physical structure of the water column of
415 ROME 2 favoured subsurface summer blooming. Furthermore, the elevated pigment concentrations also
416 extended deeper in the water column, indicating that phytoplanktonic colonies were slowly sinking in the
417 relatively non-turbulent water. This physical quietude allowed the POM to sink while maintaining the same
418 caloric content of the mixed layer, as previously found for the coastal TNB (Fabiano et al., 1996), when the
419 caloric value was on average 5.33 Kcal/g. Actually, this is not very high, due to the high contribution of
420 carbohydrates that have the lowest caloric value among the three biochemical components. We observed
421 that in ROME 2 the chlorophyll-a was associated with carbonaceous POM (it correlated positively to the
422 POC/PN ratio), therefore in this area the freshly-produced summer POM had different features, namely a
423 lower trophic value, than the offshore area.
424
425 *4.3 Hydrolysable proteins and carbohydrates of summer POM*

426 Generally, the hydrolysable protein contribution was rather low during the ROME cruise, on average 35% of
427 the total proteins. This value was clearly lower than the contribution (higher than 90%) observed at coastal
428 stations in the NW Mediterranean (Misic and Covazzi Harriague, 2008), and by Fabiano and Pusceddu
429 (1998), who observed that 60% of the total proteins in TNB were hydrolysable. Anyway, these differences
430 may be due to the fact that the cited authors used trypsin to hydrolyse proteins, while in the present study
431 we used proteinase K.
432 The contribution of the hydrolysable fraction to the POC highlighted slight but interesting differences
433 between the ROME areas and also within the same area, following the mesoscale physical features.
434 Assuming that the POM production in the Ross Sea has a main phytoplanktonic signature (Fragoso and
435 Smith, 2012), the fresh (generally more labile) POM should be found at the surface at the beginning of the
436 productive season (spring), but the POM vertical fluxes of summer and the proliferation of the bacterial
437 biomass would provide sinking particles of labile heterotrophic materials such as proteins.
438 At the ROME sites the contribution of the labile proteinaceous C to the POC and the N to the TN were,
439 generally, higher in the deeper layer than in the mixed layer (Fig. 7, related also to the hydrolysable
440 carbohydrates). In ROME 1 this was particularly true for the stations that had experienced longer ice-free
441 conditions. Generally, in ice-free areas, the relaxing of the stratification due to wind and waves allows an
442 increased vertical flux of POM in terms of quantity and also of velocity of the sinking (Hargrave et al., 2002).
443 The lower maturity of station 20 (namely a higher ice-influence as revealed by salinity), instead, led to
444 conditions more similar to spring, with a higher labile contribution at the surface.
445 ROME 2, instead, showed peculiar features. Despite being ice-free for the longest time and lying nex to the
446 winter polynya of TNB, its stations showed a lower labile contribution in the deeper layer than in the UML.
447 Station 39 was the exception, lying to the east of the hydrological front and being influenced by an offshore
448 current coming from the ROME 1 area. The other stations were separated from the actual offshore area by
449 the front found at stations 34 and 45.
450 The vertical transport of the POM has a double relevance: it is essential for the foraging of bottom and
451 mesopelagic communities, and it may contribute to the CO_2 biological pump. The occurrence of vertical

transport, as shown by the ROME 2 and coastal observations in terms of bulk POM, may improve deep sea trophism, but also push C into the deep current system via bottom-water. The vertical distribution of POM at the ROME 2 stations was encouraging, because the POM accumulation was observed down to 200 m. In fact, the TNB area is characterised by the formation of dense water masses due to brine release during sea-ice roduction (HSSW) and by the freshening and cooling of the HSSW due to contact with the ice shelf (TISW). HSSW fills-up the deeper layer of the Drygalsky Basin and flows northwards until it reaches the shelf-break, where overflows down the continental slope, ventilating to the abyssal depths near Cape Adare (Jacobs et al., 1970; Withworth and Orsi, 2006; Budillon et al., 2011).

The deep layer POM of ROME 2 was more refractory, showing proportionally lower hydrolysable proteins and carbohydrates, higher POC/PN ratio, lower protein/carbohydrate ratio and a lower caloric content than the mixed layer. If refractivity is a limiting factors for the biological respiration of POM, it allows a more efficient burial of unrespired C to the depth, indicating TNB as a sink for C in summer (Fonda Umani et al., 2002).

5. Conclusions

In this study we firstly aimed at determining whether the POM was uniformly distributed in the Ross Sea during a particular season (summer), when one of the main constraints regulating POM production and consumption (namely the ice cover) was generally lacking. We found that heterogeneity was still a dominant feature of the Ross Sea, due to the mesoscale characteristics of each area. The presence of fronts and eddies, with high current intensities, mixed the UML, stimulating phytoplanktonic production and POM accumulation. Nevertheless, the vertical and horizontal extent of this fertilisation was not continuous. The offshore ROME 1 and 3 areas differed from the ROME 2 area, especially with regards to the qualitative trophic features of the POM. The deeper-layer POM was found to have higher lability in ROME 1 and 3, while the more coastal ROME 2 had inverse features. This may be relevant, because the POM of the deeper water, which would likely join the dense-water journey to the abyssal depths of the oceans, has a potentially lower trophic value and could be respired to a lesser extent, contributing to C sinking to the bottom. On the other hand, enrichment of the deeper POM of the other areas via bacterial growth and high

protein-containing phytoplankton would increase its trophic value, providing a valuable source of materials and energy for those consumers that also maintain a certain metabolic activity during winter.

This study also highlighted that the heterogeneity of the offshore areas was principally a matter of the UML. This is a critical point, because the surface layer is the first to be influenced by climatic changes. Small atmospheric changes could lead to increased ecological changes, altering the fragile balance of the Southern Ocean.

Acknowledgements

We would like to thank the captain and crew of the R/V Italica for their unstinting assistance during the cruise. We are grateful to Paolo Povero and Enrico Olivari for their logistical support and for the hard sampling work, to Paola Rivaro, who provided the UML depths, and to Giorgio Budillon for the constructive discussion on the physical data. This study was conducted in the framework of the project "Ross Sea Mesoscale Experiment (ROME)" funded by the Italian National Program for Antarctic Research (PNRA, 2013/AN2.04).

References

Arrigo, K.R., Worthen, D., Schnell, A., Lizotte, M.P., 1998. Primary production in Southern Ocean Waters. J. Geophys. Res. 103, 15587–15600.

Arrigo, K.R., van Djiken, G.L., 2004. Annual changes in sea-ice, chlorophyll a, and primary production in the Ross Sea, Antarctica. Deep Sea Res. I 51, 117–138.

Bligh, E.G., Dyer, W.J., 1959. A rapid method of total lipid extraction and purification. Can. J. Biochem. Physiol. 37, 911–917.

Budillon, G., Spezie, G., 2000. Thermohaline structure and variability in the Terra Nova Bay polynya, Ross Sea. Antarct. Sci. 12, 493–508.

Budillon, G., Castagno, P., Aliani, S., Spezie, G., Padman, L., 2011. Thermohaline variability and Antarctic bottom water formation at the Ross Sea shelf break. Deep Sea Res. Part I, 1002–1018.

505 Budillon, G., Pacciaroni, M., Cozzi, S., Rivaro, P., Catalano, G., Ianni, C., Cantoni, C., 2003. An optimum
506 multiparameter mixing analysis of the shelf waters in the Ross Sea. Antarct. Sci. 15,105-118.
507 Carlson, C.A., Ducklow, H.W., Hansell, D.A., Smith, W.O., 1998. Organic carbon partitioning during spring
508 phytoplankton blooms in the Ross Sea polynya and the Sargasso Sea. Limnol Oceanogr. 43 (3), 275-
509 386.
510 Catalano, G., Povero, P., Fabiano, M., Benedetti, F., Goffart, A., 1997. Nutrient utilisation and particulate
511 organic matter changes during summer in the upper mixed layer (Ross Sea, Antarctica). Deep-Sea
512 Res. I 44, 97–112
513 Celussi, M., Cataletto, B., Fonda Umani, S., Del Negro, P., 2009. Depth profiles of bacterioplankton
514 assemblages and their activities in the Ross Sea. Deep-Sea Res. I 56, 2193–2205.
515 Comiso, J.C., McClain, C.R., Sullivan, C.W., Ryan, J.P., Leonard, C.L., 1993. Coastal Zone Color Scanner
516 pigment concentrations in the Southern Ocean and relationships to geophysical surface features. J.
517 Geophys. Res. 98, 2419-2451.
518 Dall, W., Moriarty, D.J.W., 1983. Functional aspects of nutrition and digestion. In: Mantel, L.H. (Ed.), The
519 Biology of Crustacea, vol. 5. Academic Press, New York, pp. 215–261.
520 Davis, J., Benner, R., 2005. Seasonal trends in the abundance, composition and bioavailability of particulate
521 and dissolved organic matter in the Chukchi/Beaufort Seas and western Canada Basin. Deep-Sea Res.
522 II 52, 3396–3410.
523 Dell'Anno, A., Fabiano, M., Mei, M.L., Danovaro, R., 2000. Enzymatically hydrolysed protein and
524 carbohydrate pools in deep-sea sediments: estimates of the potentially bioavailable fraction and
525 methodological considerations. Mar. Ecol. Progr. Ser. 196, 15–23.
526 Dubois, M., Gilles, K.A., Hamilton, J.K., Rebers, P.A., Smith, F., 1956. Colorimetric method for determination
527 of sugars and related substances. Anal. Chem. 39, 350-356.
528 Dunbar, R.B., Leventer, A.R., Mucciarone, D.A., 1998. Water column sediment fluxes in the Ross Sea,
529 Antarctica: atmospheric and sea ice forcing. J. Geophys. Res. 103 (30), 741-759.

530 Erofeeva, S.Y., Egbert, G.D., Padman L., 2005: Assimilation of ship-mounted ADCP data for barotropic tides:
531 Application to the Ross Sea, J. Atmos. Oceanic Technol., 22: 721-734.
532 Etcheber, H., Relexans, J.-C., Beliard, M., Weber, O., Buscail, R., Heussner, S., 1999. Distribution and quality
533 of sedimentary organic matter on the Aquitanian margin (Bay of Biscay). Deep-Sea Res. 46, 2249-
534 2288.
535 Fabiano, M., Pusceddu A., 1998. Total and hydrolizable particulate organic matter (carbohydrates, proteins
536 and lipids) at a coastal station in Terra Nova Bay (Ross Sea, Antarctica). Polar Biol. 19,125-132.
537 Fabiano, M., Povero, P., Danovaro, R., 1993. Distribution and composition of particulate organic matter in
538 the Ross Sea (Antarctica). Polar Biol.13, 525–533.
539 Fabiano, M., Danovaro, R., Crisafi, E., La Ferla, R., Povero, P., Acosta-Pomar, L., 1995. Particulate matter
540 composition and bacterial distribution in Terra Nova Bay (Antarctica) during summer 1989-1990.
541 Polar Biol. 15, 393-400.
542 Fabiano, M., Povero, P., Danovaro, R., 1996. Particulate organic matter composition in Terra Nova Bay (Ross
543 Sea, Antarctica) during summer 1990. Antarct. Sci. 8, 7–13.
544 Fabiano, M., Chiantore, M., Povero, P., Cattaneo-Vietti, R., Pusceddu, A., Misic, C., Albertelli, G., 1997.
545 Short-term variation in particulate matter flux in Terra Nova Bay, Ross Sea. Antarct. Sci. 9, 143-149.
546 Fabiano, M., Povero, P., Misic, C. 2000. Spatial and temporal distribution of particulate organic matter in
547 the Ross Sea. In Faranda, F.M., Guglielmo, L., Ianora, A. (Eds.) Ross Sea ecology. Berlin: Springer, pp.
548 135–150.
549 Fitch, D. T., Moore, J. K., 2007. Wind speed influence on phytoplankton bloom dynamics in the Southern
550 Ocean Marginal Ice Zone, J. Geophys. Res. 112, C08006, doi:10.1029/2006JC004061.
551 Fonda Umani, S., Accornero, A., Budillon, G., Capello, M., Tucci, S., Cabrini, M., Del Negro, P., Monti, M., De
552 Vittor, C., 2002. Particulate matter and plankton dynamics in the Ross Sea Polynya of Terra Nova Bay
553 during the austral summer 1997/1998. J. Mar. Syst. 36, 29–49.
554 Fragoso, G.M., Smith Jr., W.O., 2012. Influence of hydrography on phytoplankton distribution in the
555 Amundsen and Ross Seas, Antarctica. J. Mar. Syst. 89, 19–29.

556 Gardner, W.D., Richardson, M.J., Smith Jr., W.O., 2000. Seasonal patterns of water column particulate
557 organic carbon and fluxes in the Ross Sea, Antarctica. Deep-Sea Res. 47, 3423-3449.
558 Garrity, C., Ramseier, R.O., Peinert, R., Kern, S., Fischer, G., 2005. Water column particulate organic carbon
559 modeled fluxes in the ice-frequented Southern Ocean. J. Mar. Syst. 56, 133– 149.
560 Gordon Jr., D.C., 1970. Some studies on the distribution and composition of particulate organic carbon in
561 the North Atlantic Ocean. Deep-Sea Res. 17, 233–243.
562 Holm-Hansen, O., Lorenzen, C.J., Holmes, R.W., Strickland, J.D.H., 1965. FluoROMEtric determination of
563 chlorophyll. J. Cons. Perm. Int. Explor. Mer. 30, 3-15.
564 Mayer, L.M., Schick, L.L., Sawyer, T., Plante, C.J., Jumars, P.A., Self, R.L., 1995. Bioavailable amino acids in
565 sediments: a biomimetic, kinetics, based approach. Limnol. Oceanogr. 40, 511–520.
566 Nelson, D.M., Demaster, D.J., Dunbar, R.B., Smith Jr., W.O., 1996. Cycling of organic carbon and biogenic
567 silica in the Southern Ocean: estimates of water-column and sedimentary fluxes on the Ross Sea
568 continental shelf. J. Geophys. Res. 10, 18519–18532.
569 Hargrave, B.T., Walsh, I.D., Murray, D.W., 2002. Seasonal and spatial patterns in mass and organic matter
570 sedimentation in the North Water. Deep-Sea Res. II 49, 5227-5244.
571 Hartree, E.F., 1972. Determination of proteins: a modification of the Lowry method that gives a linear
572 photometric response. Anal. Biochem. 48, 422–427.
573 Hedges, J.I., Stern, J.H., 1984. Carbon and nitrogen determination of carbonate-containing solids. Limnol.
574 Oceanogr. 29, 657–663.
575 Huston, A.L., Deming, J.W., 2002. Relationships between microbial extracellular enzymatic activity and
576 suspended and sinking particulate organic matter: seasonal transformations in the North Water.
577 Deep-Sea Res. II 49, 5211–5225.
578 Jacobs, S.S., Amos, A.F., Bruchhausen, P.M., 1970. Ross Sea oceanography and Antarctic Bottom Water
579 formation. Deep-Sea Res. 17, 935–962.

580 Kim, B.K., Lee, J.H., Yun, M.S., Joo, H.T., Song, H.J., Yang, E.J., Chung, K.H., Kang, S.-H., Lee, S.H., 2014. High
581 lipid composition of particulate organic matter in the northern Chukchi Sea, 2011. Deep- Sea Res. II,
582 120, 72-81. DOI: 10.1016/j.dsr2.2014.03.022i
583 Kirchman, D.L., Meon, B., Ducklow, H.W., Carlson, C.A., Hansell, D.A., Steward, G.F., 2001. Glucose fluxes
584 and concentrations of dissolved combined neutral sugars (polysaccharides) in the Ross Sea and Polar
585 Front Zone, Antarctica. Deep-Sea Res. II 48, 4179–4197.
586 Marsh, J.B., Weinstein, D.B., 1966. A simple charring method for determination of lipids. J. Lipid Res. 7, 574-
587 576.
588 Mayer, L.M., Schick, L.L., Sawyer, T., Plante, C.J., Jumars, P.A., Self, R.L., 1995. Bioavailable amino acids in
589 sediments: a biomimetic, kinetics, based approach. Limnol. Oceanogr. 40, 511–520.
590 Misic, C., Covazzi Harriague, A., 2008. Organic matter recycling in a shallow coastal zone (NW
591 Mediterranean): the influence of local and global climatic forcing and organic matter lability on
592 hydrolytic enzyme activity. Cont. Shelf Res. 28, 2725-2735.
593 Misic, C., Fabiano, M., 1996. A functional approach to the assessment of the nutritional value of the
594 particulate organic matter. Chem. Ecol. 13, 51–63.
595 Misic, C., Povero, P., Fabiano, M., 2002. Ectoenzymatic ratios in relation to particulate organic matter
596 distribution (Ross Sea, Antarctica). Microb. Ecol. 44, 224–234.
597 Orsi, A.H., Wiederwohl, C.L., A recount of Ross Sea waters. Deep-Sea Research II (2009), doi:10.1016/
598 j.dsr2.2008.10.033
599 Povero, P., Chiantore, M., Misic, C., Budillon, G., Cattaneo-Vietti, R., 2001. Land forcing controls pelagic-
600 benthic coupling in Adélie Cove (Terra Nova Bay, Ross Sea). Polar Biol. 24, 875–882.
601 Povero, P., Misic, C., Ossola, C., Castellano, M., Fabiano, M., 2003. The trophic role and ecological
602 implications of oval faecal pellets in Terra Nova Bay (Ross Sea). Polar Biol. 26, 302–310.
603 Rigual-Hernández, A.S., Trull, T.W., Bray, S.G., Closset, I., Armand, L.K., 2015. Seasonal dynamics in diatom
604 and particulate export fluxes to the deep sea in the Australian sector of the southern Antarctic Zone.
605 J. Mar. Syst. 142, 62–74.

606 Rivaro, P., Messa, R., Ianni, C., Magi, E., Budillon, G., 2014. Distribution of total alkalinity and pH in the Ross
607 Sea (Antarctica) waters during austral summer 2008. Polar Research 33,
608 20403,http://dx.doi.org/10.3402/polar.v33.20403.
609 Rivaro, P., Ianni, C., Langone, L., Ori, C., Aulicino, G., Cotroneo, Y., Saggiomo, M., Mangoni O., this issue.
610 Physical and biological forcing on the mesoscale variability of the carbonate system in the Ross Sea
611 (Antarctica) during the summer season 2014. J. Mar. Syst., in press.
612 Saggiomo, V., Carrada, G.C., Mangoni,O., Ribera d'Alcalà, M., Russo A., 1998. Spatial and temporal
613 variability of size-fractionated biomass and primary production in the Ross Sea (Antarctica) during
614 austral spring and summer. J Mar. Syst. 17, 115–127.
615 Sala, M.M., Arin, L., Balagué, V., Felipe, J., Guadayol, Ò., Vaqué, D., 2005. Functional diversity of
616 bacterioplankton assemblages in western Antarctic seawaters during late spring. Mar. Ecol. Prog. Ser.
617 292, 13–21.
618 Smith Jr, W.O., Nelson, D.M., Di Tullio, G.R., Leventer, A.R., 1996.Temporal and spatial patterns in the Ross
619 Sea: phytoplankton biomass elemental composition, productivity and growth rates. J. Geophys. Res.
620 101, 18455–18466.
621 Smith Jr., W.O., Asper, V.A., 2001. The influence of phytoplankton assemblage composition on
622 biogeochemical characteristic and cycles in the Southern Ross Sea, Antarctica. Deep Sea Res. I 48,
623 137–161.
624 Smith Jr., W.O., Marra, J., Hiscock, M.R., Barber, R.T., 2000. The seasonal cycle of phytoplankton biomass
625 and primary productivity in the Ross Sea, Antarctica. Deep Sea Res. II 47, 3119–3140.
626 Spreen, G., L. Kaleschke, and G. Heygster(2008), Sea ice remote sensing using AMSR-E 89 GHz channels *J.*
627 *Geophys. Res.*, vol. 113, C02S03, doi:10.1029/2005JC003384.
628 Winberg, G.G., 1971. Symbols, units and conversion factors in study of fresh waters productivity. Int. Biol.
629 Programme, 23.
630 Whitworth T., III, Orsi, A.H., 2006. Antarctic Bottom Water production and export by tides in the Ross Sea,
631 Geophys. Res. Lett. 33, L12609,doi:10.1029/2006GL026357

632 Young, J.N., Goldman, J.A.L., Kranz, S.A., Tortell, P.D., Morel, F.M.M., 2015. Slow carboxylation of Rubisco
633 constrains the rate of carbon fixation during Antarctic phytoplankton blooms. New Phytol. 205, 172–
634 181. doi: 10.1111/nph.13021

635 **Captions to figures**

636

637 Fig. 1. A: Map of the stations of the ROME 1 (red dots), ROME 2 (blue dots) and ROME 3 (green dots) areas.
638 Black-circled points indicate the POM sampling stations. B: Θ/S diagram obtained from the entire available
639 dataset indicates the main water masses. Data from the three different areas (ROME 1, ROME 2 and ROME
640 3) are represented with different colours (red, blue and green, respectively).

641

642 Fig. 2. Sea-ice concentration maps of the Ross Sea for 1 December (A), 19 December (B), 7 January (C), 14
643 January (D). Red circles and numbers highlight the position of the ROME 1, ROME 2 and ROME 3 sampling
644 areas.

645

646 Fig. 3. Station map (A) and maps of mean salinity (B), temperature (C) and currents (D) in the upper mixed
647 layer at ROME 1.

648

649 Fig. 4. Station map (A) and maps of mean salinity (B), temperature (C) and currents (D) in the upper mixed
650 layer at ROME 2.

651

652 Fig. 5. Station map (A) and maps of mean salinity (B), temperature (C) and currents (D) in the upper mixed
653 layer at ROME 3.

654

655 Fig. 6. Vertical profiles of the variables averaged for each depth at each area (standard deviations are
656 reported). A: particulate organic carbon (POC), B: particulate nitrogen (PN), C: particulate organic
657 carbon/particulate nitrogen ratio (POC/PN), D: particulate proteins (PRT), E: hydrolysable particulate
658 proteins (h-PRT), F: particulate proteins/carbohydrate ratio (PRT/CHO), G: particulate carbohydrates (CHO),
659 H: hydrolysable particulate carbohydrates (h-CHO), I: particulate lipids (LIP).

660

661 Fig. 7. Average contribution of the hydrolysable fraction of proteins and carbohydrates to the POC in the
662 three areas. Standard deviations are reported. Grey: UML, black: deeper layer.
663
664 Fig. 8. PCA for the entire ROME cruise and for the previous studies in the upper mixed layer (UML, coloured
665 markers) and deeper layer (DL, blue markers). Two main groups (A and B) are composed of the four sub-
666 groups a1 and a2 (A), b1 and b2 (B). The ellipses are drawn following the results of the cluster analysis on
667 the normalised data (Euclidean distance = 1.8). See text and Table 2 for details. The vectors of the variables
668 are reported on the upper left of the plot.
669
670 Fig. 9. Plot of the POC concentration and caloric value of the POM for the upper mixed layer (A) and the
671 deeper layer (B). Black numbers and markers refer to the previous studies in the Ross Sea and coastal Terra
672 Nova Bay (TNB), red numbers and markers refer to the ROME cruise results. Coloured boxes group the
673 stations that have similar ice-related features (blue: pack-ice coverage, green: marginal ice zone – MIZ, red:
674 polynya) or belong to the coastal sites (violet). See Table 2 for details.

675 Table 1. Position of the stations sampled for POM characterisation during the ROME cruise in 2014, depth of the
676 upper mixed layer (UML) and number of sampled depths for each station.

677

	station	date	longitude (°E)	latitude (°S)	UML depth (m)	sampled depths
ROME 1	9	16 Jan	173.87	75.00	38	5
	11	16 Jan	172.03	75.00	29	5
	13	16 Jan	170.76	75.00	32	5
	16	17 Jan	169.50	74.83	15	5
	18	17 Jan	169.51	74.51	17	5
	20	17 Jan	169.88	73.99	14	5
ROME 2	33	26 Jan	166.06	74.70	18	4
	34	26 Jan	165.75	74.76	13	5
	36	27 Jan	165.18	74.88	12	5
	39	27 Jan	166.06	74.86	24	4
	43	27 Jan	164.98	74.79	14	4
	45	28 Jan	165.49	74.82	15	5
ROME 3	48	31 Jan	167.83	76.40	33	5
	50	31 Jan	168.65	76.40	36	5
	52	1 Feb	169.53	76.42	75	4
	55	1 Feb	168.40	76.43	44	5
	56	1 Feb	168.16	76.54	12	5
	65	2 Feb	169.58	76.50	115	4
	67	2 Feb	168.72	76.50	51	5
	69	2 Feb	168.01	76.50	14	4
	75	3 Feb	168.80	76.38	42	5

678

679 Table 2. Features of the stations sampled during previous researches, here used as a comparison for the ROME
680 cruise observations.
681

area	season	environmental features	station	lat °S	long °E	reference
Ross Sea	spring	polynya	MP	76.50	175.00	Fabiano et al. (2000)
		MIZ	8	75.16	175.18	
		MIZ	10	74.84	174.88	
		MIZ	28	74.70	172.01	
		MIZ	30	74.69	164.18	
		pack	27	71.94	174.98	
		pack	29	74.98	167.99	
	early summer	polynya	15	72.35	179.78	Fabiano et al. (1993); Catalano et al. (1997)
		polynya	17	73.23	179.84	
		polynya	19	74.95	179.82	
		polynya	21	74.98	174.87	
		MIZ	23	74.99	170.00	
		MIZ	25	74.95	165.25	
Terra Nova Bay	summer	coastal-open waters	TNB	74.78	164.17	Povero et al. (2001)
			TNBa	74.75	164.17	Fabiano et al. (1995)
			TNBb	74.70	164.13	Fabiano et al. (1997)

682

683 Table 3. Average data and standard deviation (sd) for the upper mixed layer (UML) and the deeper layer (DL) of the ROME 1, ROME 2 and ROME 3 stations.

position	station	water	Chl-a		PN		POC		PRT		h-PRT		CHO		h-CHO		LIP		POC/Chl-a		POC/PN		PRT/CHO	
		layer	µg/l	sd	µg/l	sd	µg/l	sd	µg/l	sd	µg/l	sd	µg/l	sd	µg/l	sd	µg/l	sd		sd		sd		sd
ROME 1	9	UML	1.62	0.06	48.7	2.1	297.3	13.7	319.7	3.9	84.2	1.1	96.7	15.0	7.4	8.8	80.6	17.2	184.2	15.3	6.1	0.0	3.3	0.5
		DL			6.7	6.5	48.5	39.5	47.6	47.9	18.4	14.2	21.6	13.4	5.0	2.1	18.3	18.6			8.0	2.4	1.9	1.0
	11	UML	1.66	0.14	50.3	5.5	290.5	19.2	324.4	23.8	78.0	1.6	123.7	24.3					174.8	2.7	5.8	0.3	2.7	0.3
		DL			5.9	3.5	39.6	15.6	49.4	17.4	17.1	6.6	16.3	5.9							7.4	1.6	3.1	1.2
	13	UML	2.02	0.35	44.9	15.9	275.1	98.0	335.3	116.1	116.1	65.1	108.5	52.3	18.3	21.8	67.7	22.6	133.7	25.3	6.1	0.0	3.2	0.5
		DL			4.7	3.3	40.3	30.2	45.1	34.3	19.3	16.7	22.5	11.9	4.0	3.0	14.8	13.6			6.8	0.8	1.9	0.6
	16	UML	2.99	0.04	48.5	41.1	301.0	202.5	333.6	225.8	105.4	44.1	118.9	82.1	13.8	16.3	67.1	5.1	101.2	69.1	5.6	0.2	2.8	0.0
		DL			4.3	2.0	32.3	19.3	34.1	34.3	15.9	15.2	19.1	6.3	2.6	1.9	5.6	4.9			6.6	0.4	1.5	1.1
	18	UML	1.50	0.22	38.1	15.8	208.1	97.3	240.7	107.4	69.9	39.1	63.7	45.3					144.9	86.2	5.5	0.2	4.3	1.3
		DL			4.4	1.8	27.1	8.5	27.0	10.4	8.6	4.4	9.6	2.2							6.3	0.7	2.8	0.5
	20	UML	2.32	0.16	18.3	0.7	112.4	4.3	134.7	15.8	44.6	1.3	52.6	6.2	2.5	1.2	27.5	9.4	48.5	1.5	5.7	0.6	2.6	0.6
		DL			2.7	1.7	21.6	11.4	15.7	15.3	5.6	6.1	12.8	4.1	1.4	1.5	9.4	2.8			7.3	0.3	1.1	0.8
ROME 2	33	UML	1.10	0.04	34.0	5.7	192.3	36.7	226.5	63.8	76.0	18.6	87.8	42.1					174.0	27.2	5.7	0.2	2.7	0.6
		DL			11.4	4.2	70.2	25.5	63.1	28.0	24.1	9.1	23.3	7.0							6.2	0.0	2.6	0.4
	34	UML	2.63	0.10	26.9	8.7	195.0	16.9	206.0	49.7	79.1	14.2	128.0	32.3	17.9	10.4	49.3	2.6	74.4	9.2	6.5	0.4	1.7	0.8
		DL			18.7	5.9	145.5	57.1	136.7	62.6	54.4	28.0	98.6	63.0	16.8	24.4	22.0	12.9			7.4	0.7	1.5	0.4
	36	UML	2.18	0.36	36.1	2.7	212.9	20.2	242.1	2.6	77.5	6.1	68.6	3.1					117.5	64.1	5.9	0.1	3.5	0.1
		DL			16.1	11.9	129.2	92.2	95.8	61.6	29.4	17.1	54.5	40.6							8.0	0.8	1.8	0.5
	39	UML	1.00	0.06	43.1	1.1	233.5	1.2	277.3	16.7	86.7	11.9	104.2	11.8	23.5	5.0	32.5	12.1	232.9		5.4	0.1	2.7	
		DL			15.2	9.0	108.3	74.0	115.3	79.8	52.5	30.6	76.3	61.7	7.9	6.1	23.2	18.5			6.7	1.0	1.6	0.2
	43	UML	1.52	0.12	38.6	3.6	233.5	0.4	306.7	36.8	97.1	11.8	102.5	9.2					153.5		6.1	0.6	3.0	
		DL			14.3	10.5	100.0	74.2	115.5	104.5	41.1	39.3	62.9	47.8							7.0	0.1	1.7	0.3
	45	UML	1.30	0.14	33.5	0.7	200.8	4.6	259.2	16.6	102.5	6.0	109.0	21.8	3.3	0.4	14.9	3.9	154.4		6.0	0.0	2.4	
		DL			24.4	14.7	162.6	97.5	174.5	123.5	64.9	39.6	111.6	81.4	8.7	12.2	16.0	12.2			6.9	0.6	1.5	0.5
ROME 3	48	UML	3.01	0.16	46.7	5.3	248.4	19.3	304.5	4.9	84.1	5.7	69.2	21.2					82.5	1.9	5.3	0.2	4.6	1.3
		DL			4.7	2.4	31.9	15.8	28.0	13.8	9.5	4.6	9.6	1.8							6.9	0.4	2.8	0.9
	50	UML	3.04	0.09	44.6	1.4	263.4	8.8	298.3	9.3	79.9	5.5	102.5	4.3	14.5	12.1	52.6	16.4	86.8	5.5	5.9	0.4	2.9	0.0
		DL			8.7	8.5	62.1	54.6	72.8	72.2	34.5	31.2	24.4	16.5	2.8	2.2	17.5	20.5			7.8	0.9	2.7	1.3
	52	UML	1.09	0.05	26.2	5.3	160.9	11.0	183.6	22.2	57.5	3.0	49.1	7.3					148.1	3.6	6.3	1.7	3.8	0.1
		DL			2.6	0.6	23.4	1.7	23.3	1.1	9.5	2.1	6.8	0.1							9.5	1.9	3.4	0.2
	55	UML	3.16	2.19	42.1	24.6	252.7	130.7	305.0	184.3	106.9	51.0	103.8	69.3	24.3	18.5	78.4	16.6	103.7	51.6	5.8	0.1	3.3	0.9
		DL			3.6	0.7	23.8	1.2	21.0	2.7	13.6	0.9	11.9	0.9	0.3	0.0	10.5	1.1			6.0	0.2	1.8	0.4
	56	UML	2.71	1.92	45.7	9.8	245.1	65.7	332.6	75.2	91.6	21.0	64.7	30.3					109.2	53.1	5.3	0.3	5.5	1.4
		DL			10.2	11.5	57.1	53.8	75.8	87.4	24.8	30.6	17.6	15.6							6.7	1.8	3.7	1.2
	65	UML	1.10	0.00	22.7	0.1	123.9	12.6	158.4	13.9	30.2	23.7	41.0	1.2					112.2	11.0	5.5	0.6	3.9	0.2
		DL			5.8	2.8	34.4	15.5	42.3	23.6	15.7	7.9	12.1	5.0							6.0	0.2	3.4	0.6
	67	UML	3.64	0.64	45.1	14.2	254.6	77.9	327.0	79.7	95.9	11.7	94.3	42.5	6.3	5.1	70.0	26.0	68.8	10.2	5.7	0.2	3.8	1.2
		DL			4.5	0.8	35.0	8.4	33.0	12.4	13.8	3.1	18.1	7.4	2.6	0.1	15.4	0.8			6.1	0.5	1.8	0.1
	69	UML	2.14	0.12	27.6	1.9	175.2	25.0	199.6	11.3	48.1	31.8	53.4	5.7					81.8	7.1	6.3	0.4	3.7	0.2
		DL			7.9	6.9	49.5	32.7	73.1	58.3	21.6	14.2	13.6	8.4							7.3	2.3	5.0	1.2
	75	UML	4.03	1.02	51.9	14.3	286.7	76.2	366.5	94.0	90.0	10.8	85.8	37.0					70.9	1.3	5.5	0.1	4.5	0.9
		DL			4.0	1.2	27.5	2.0	22.7	9.1	8.2	6.2	6.8	1.5							7.2	1.6	3.3	0.6

Chl: chlorophyll-a, PN: particulate nitrogen, POC: particulate organic carbon, PRT: particulate proteins, h-PRT: hydrolysable particulate proteins, CHO: particulate carbohydrates, h-CHO: hydrolysable particulate carbohydrates, LIP: lipids, POC/Chl: POC/chlorophyll-a ratio, PRT/CHO: protein/carbohydrate ratio, POC/PN: POC/PN ratio.

Table 4. Significant correlations between the different variables for each area investigated during the ROME cruise. Underlined numbers: p<0.05, normal numbers: p<0.01, bold numbers: p<0.001. The number of observation varied in the three Legs and depending on the variable: in ROME 1 chlorophyll-a showed 13 observations, hydrolysable carbohydrate and lipid 18, the other variables 28. In ROME 2 they were: 19, 12 and 25, respectively. In ROME 3: 25, 13 and 40, respectively. Abbreviations as in Table 2.

		chl	TN	POC	prt	h-PRT	CHO	h-CHO
ROME 1	TN	0.68						
	POC	0.72	**1.00**					
	prt	0.73	**0.99**	**1.00**				
	h-PRT	0.76	**0.94**	**0.95**	**0.97**			
	CHO	0.71	**0.97**	**0.98**	**0.98**	**0.94**		
	h-CHO	-	**0.76**	**0.75**	**0.77**	**0.83**	**0.82**	
	LIP	*0.63*	**0.89**	**0.92**	**0.91**	**0.90**	**0.88**	0.65

		chl	TN	POC	prt	h-PRT	CHO	h-CHO
ROME 2	TN	-						
	POC	-	**0.96**					
	prt	-	**0.97**	**0.95**				
	h-PRT	-	**0.89**	**0.90**	**0.94**			
	CHO	0.65	**0.68**	**0.81**	**0.77**	**0.79**		
	h-CHO	-	-	-	-	-	0.72	
	LIP	-	-	-	-	-	*0.53*	*0.63*

		chl	TN	POC	prt	h-PRT	CHO	h-CHO
ROME 3	TN	**0.95**						
	POC	**0.95**	**0.99**					
	prt	**0.95**	**0.99**	**0.99**				
	h-PRT	**0.86**	**0.93**	**0.94**	**0.94**			
	CHO	**0.90**	**0.93**	**0.95**	**0.94**	**0.91**		
	h-CHO	*0.64*	0.74	0.74	0.74	0.72	**0.80**	
	LIP	0.68	**0.91**	**0.91**	**0.90**	**0.90**	**0.89**	0.68

693 Table 5. Multivariate statistical analysis (ANOSIM and SIMPER) for the two main groups A and B of the PCA
694 (Fig. 8) and the sub-groups a1-a2 and b1-b2. Mean values ± standard deviation for each group and sub-
695 group are reported (POC, PRT and CHO: µg l^{-1}; PRT/CHO: µg $µg^{-1}$). Abbreviations as in Table 2.

696

ANOSIM

sub-groups	R statistic	significance %
A vs B	0.847	0.1
a1 vs a2	0.656	0.1
b1 vs b2	0.903	0.1

697

SIMPER

groups	variable	%		average±sd		average±sd
A vs B	PRT	32	A:	281.4±62.9	B:	58.8±47.5
	PRT/CHO	25		3.6±1.0		2.1±0.9
	CHO	24		90.0±32.9		32.7±30.0
	POC	19		242.8±55.0		72.4±53.9
a1 vs a2	PRT/CHO	41	a1:	4.3±0.7	a2:	2.9±0.4
	CHO	36		63.1±15.7		115.1±23.0
	PRT	14		243.8±60.1		316.4±43.0
b1 vs b2	CHO	47	b1:	15.9±5.5	b2:	71.5±27.1
	PRT/CHO	22		2.2±1.0		1.7±0.4
	POC	17		40.7±14.4		145.7±36.6
	PRT	14		33.2±17.1		118.0±41.8

698

Figure 1

Click here to download high resolution image

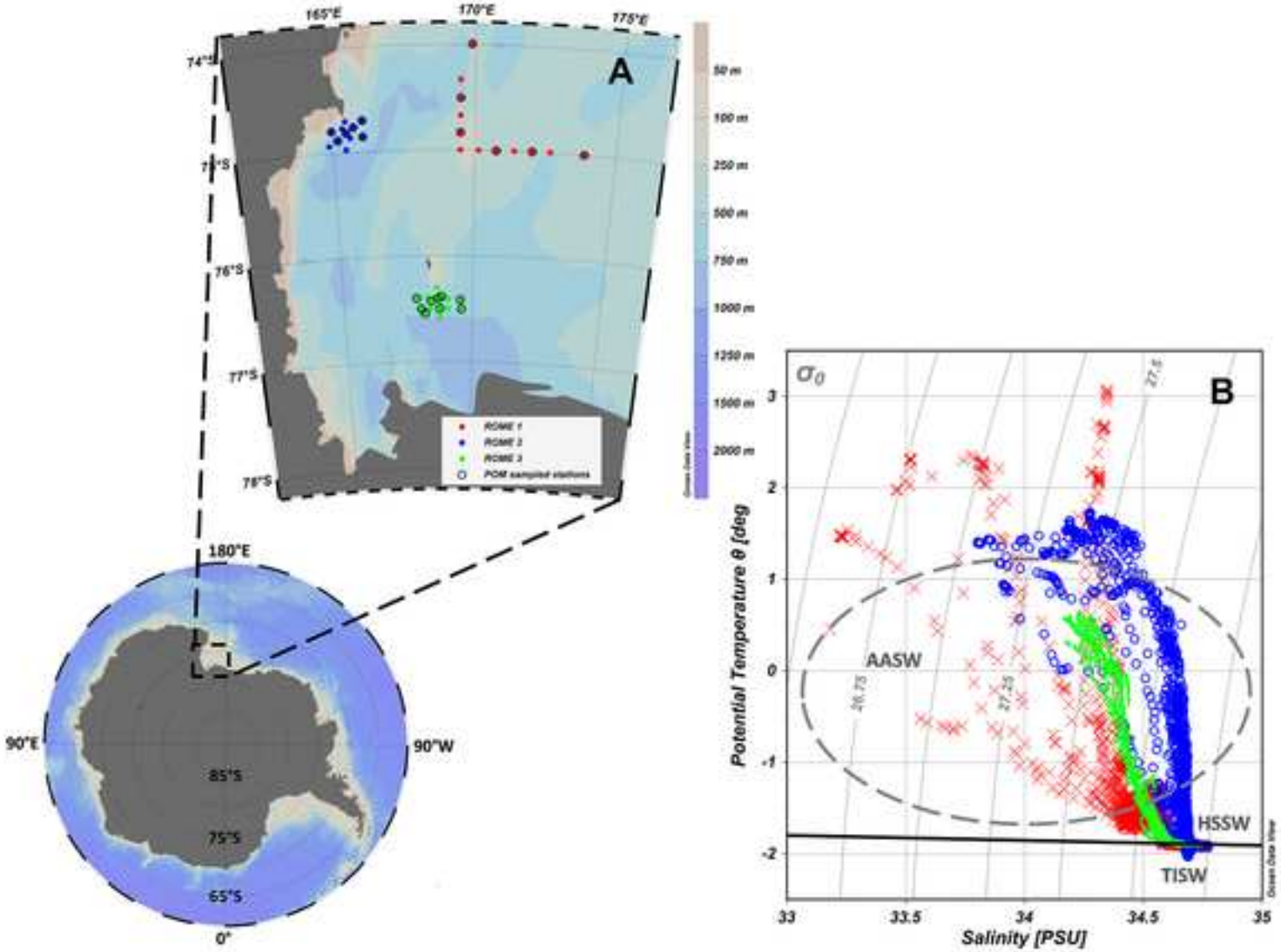

Figure 2

Click here to download high resolution image

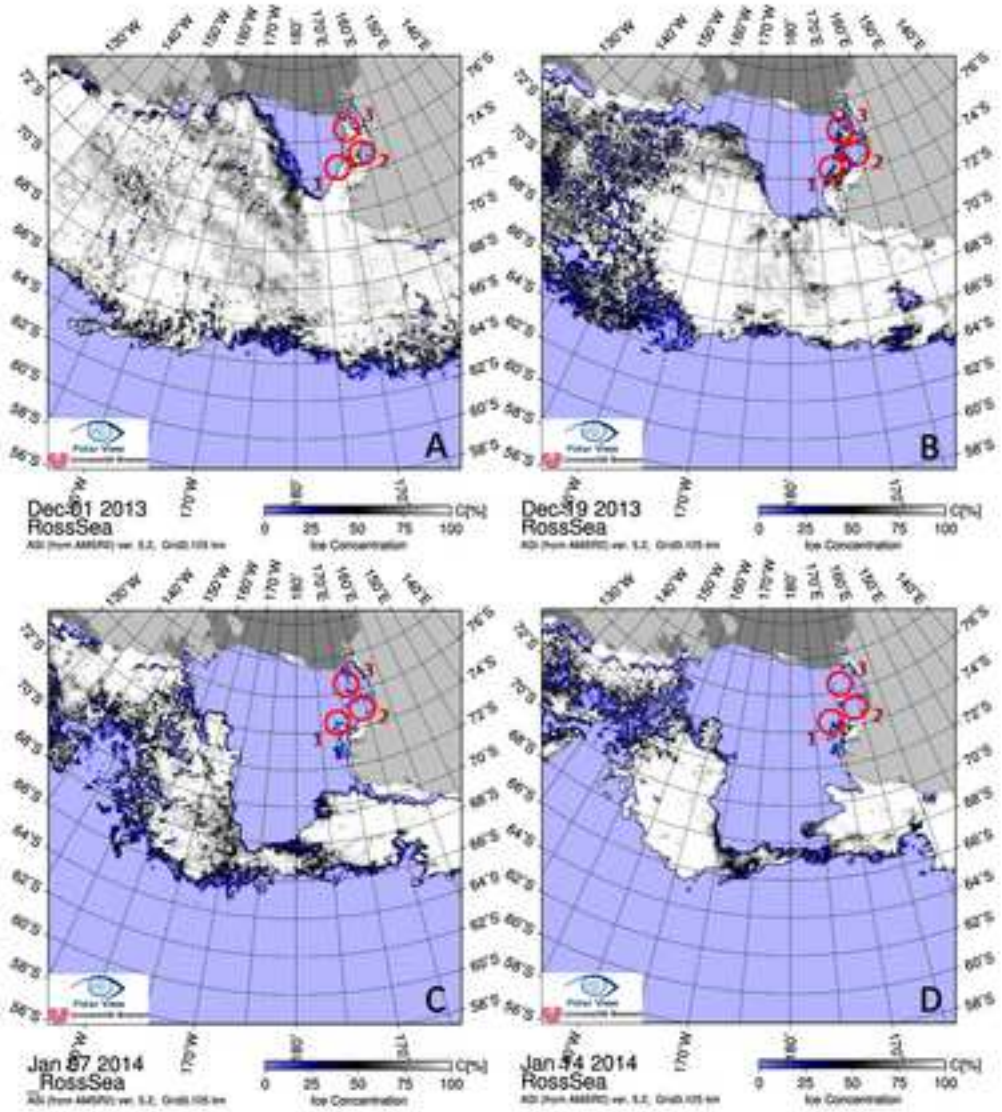

Figure 3

Click here to download high resolution image

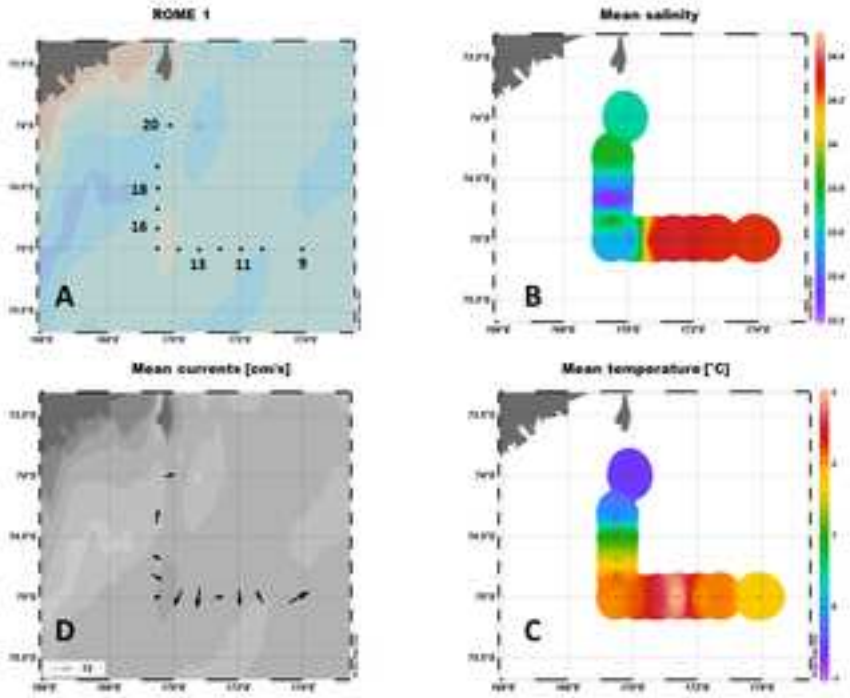

Figure 4

Click here to download high resolution image

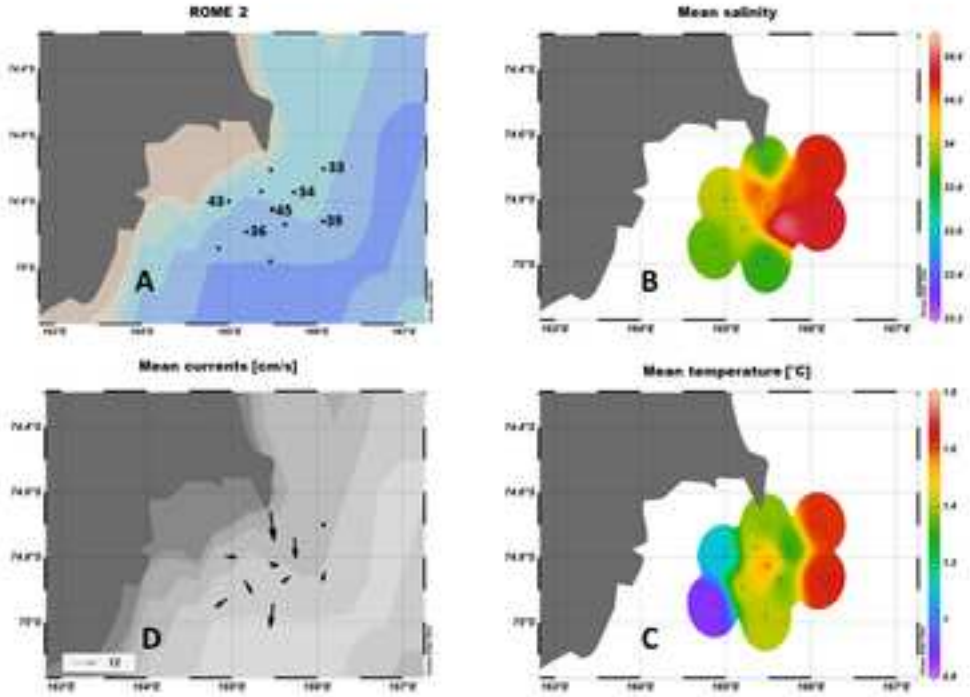

Figure 5

Click here to download high resolution image

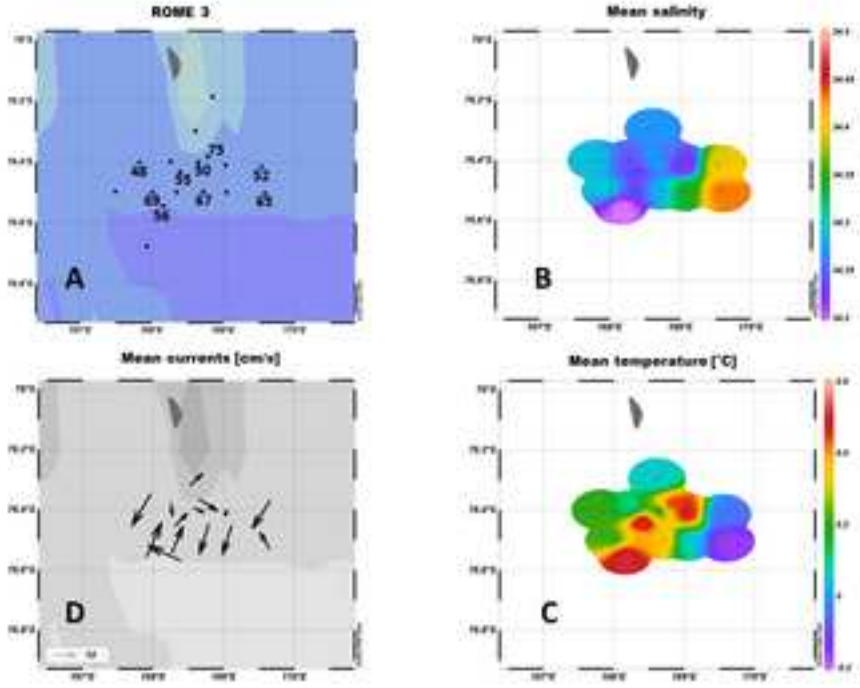

Figure 6

Click here to download high resolution image

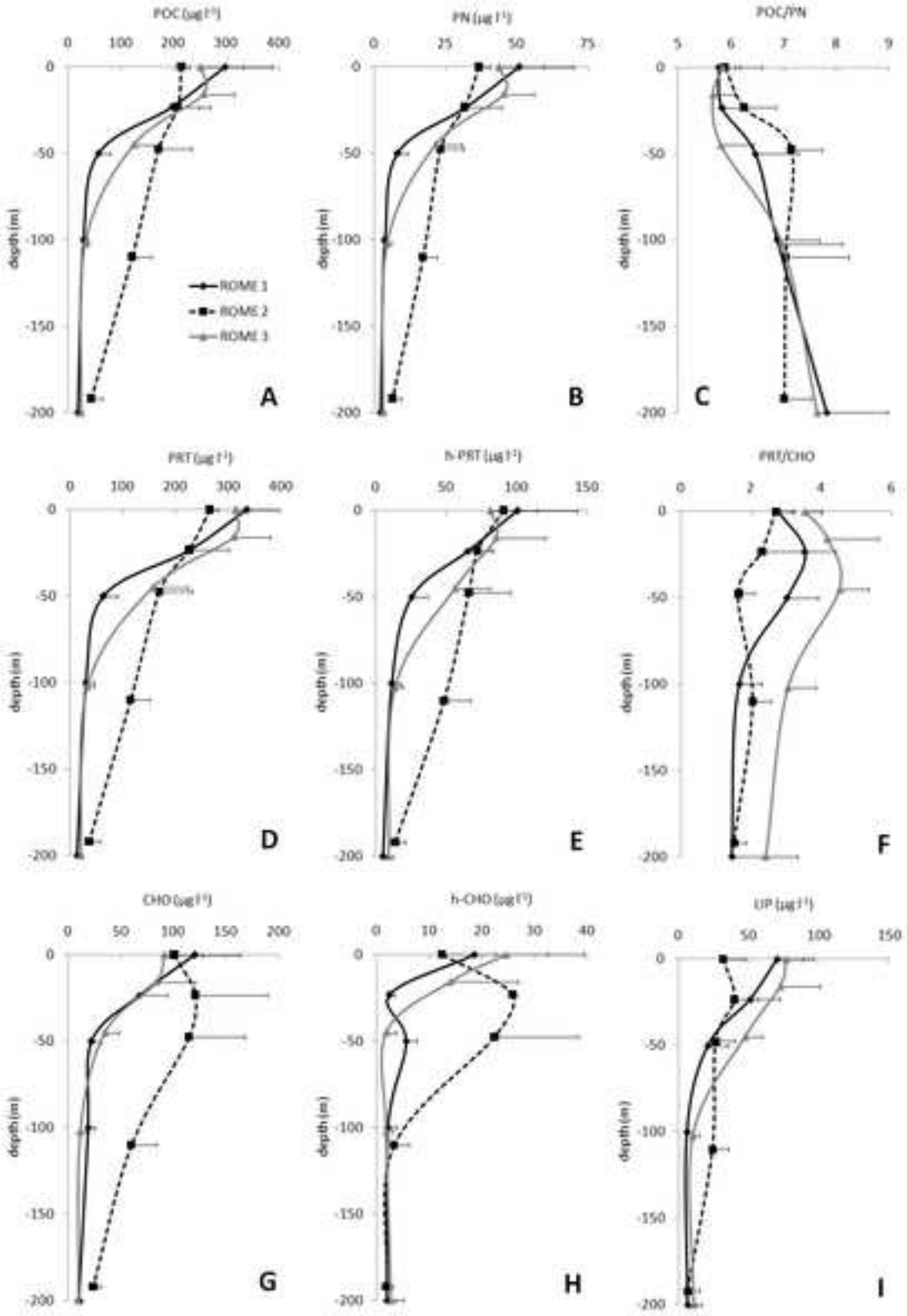

Figure 7

Click here to download high resolution image

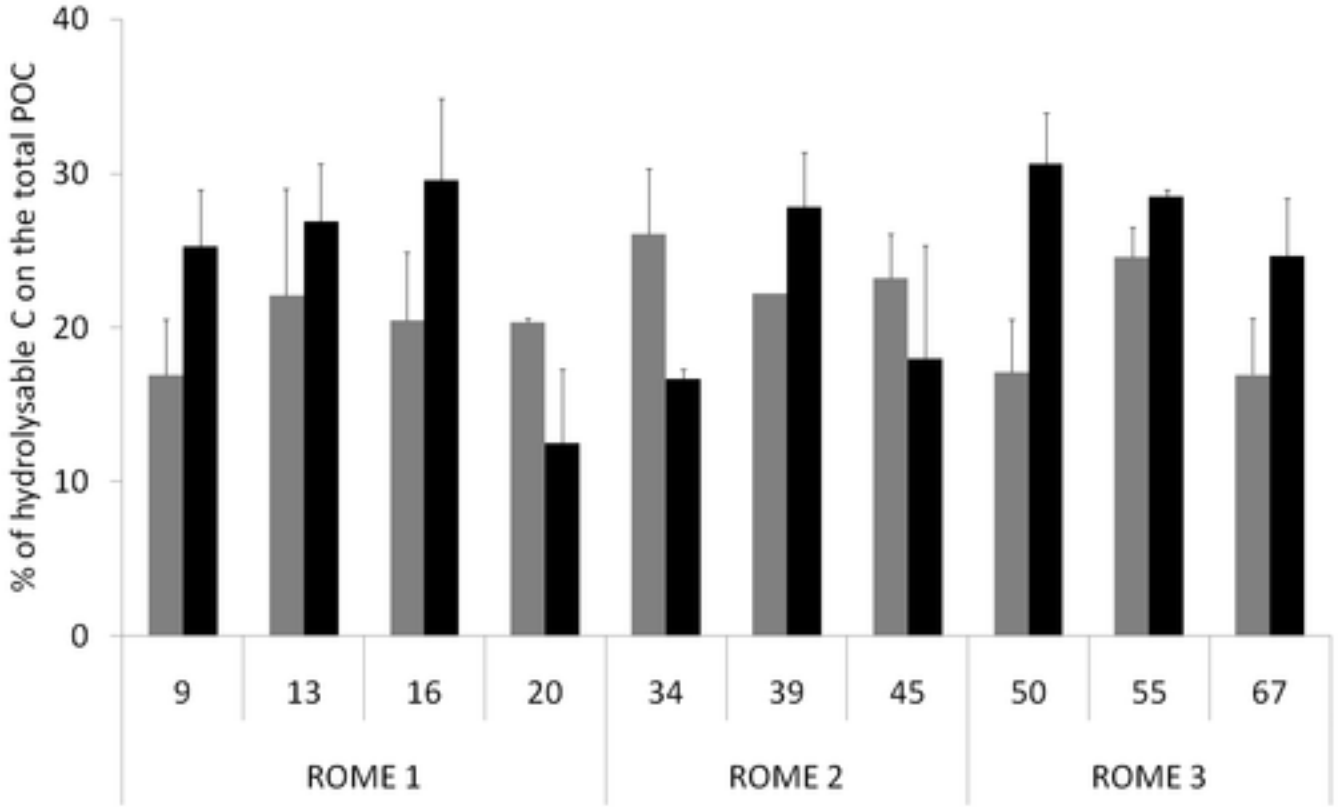

Figure 8

Click here to download high resolution image

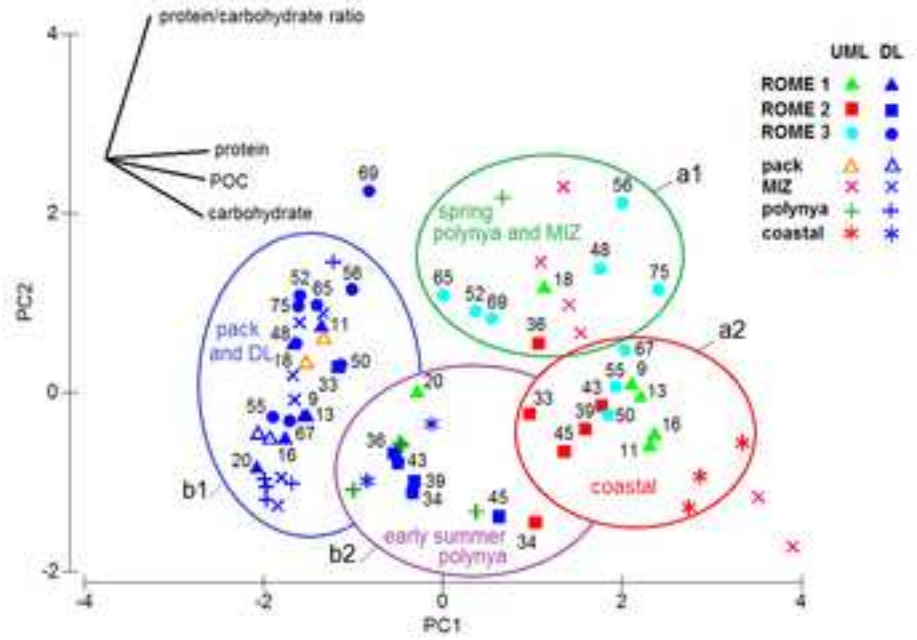

Figure 9

Click here to download high resolution image